Ficus Carica Mediated Synthesis of Simulated Solar Light Driven Nano-sized Zinc Stannate Photocatalyst for the Degradation of Methylene Blue

Asia Naqeeb
University of Azad Jammu and Kashmir

Sirajul Haq (✉ cii_raj@yahoo.com)
University of Azad Jammu and Kashmir   https://orcid.org/0000-0002-9424-2531

Rimsha Ehsan
University of Azad Jammu and Kashmir

Muhammad Imran Shahzad
National Center for Physics (NCP)

Nadia Shahzad
National University of Science and Technology (NUST)

Wajid Rehman
Hazara University Mansehra

Muhammad Waseem
COMSATS University Islamabad (CUI)

Pervaiz Ahmad
University of Azad Jammu and Kashmir

Umedjon Khalilov
University of Antwerp and Academy of Sciences of the Republic of Uzbekistan

---

Research Article

Ficus carica mediated synthesis of simulated solar light driven nano-sized zinc stannate photocatalyst for the degradation of methylene blue

Asia Naqeeb[1], Sirajul Haq[1*], Rimsha Ehsan[1], Muhammad Imran Shahzad[2], Nadia Shahzad[3], Wajid Rehman[4], Muhammad Waseem[5], Pervaiz Ahmad[6], Umedjon Khalilov[7,8]

[1]Department of Chemistry, University of Azad Jammu and Kashmir, Muzaffarabad, 13100 Pakistan.

[2]Nanosciences and Technology Department (NS & TD), National Center for Physics (NCP), 44000 Islamabad, Pakistan.

[3]US-Pakistan Centre for Advanced Studies in Energy, National University of Science and Technology (NUST), 44000 Islamabad, Pakistan.

[4]Department of Chemistry, Hazara University Mansehra, 21300 Pakistan.

[5]Department of Chemistry, COMSATS University Islamabad (CUI), Islamabad Pakistan.

[6]Department of Physics, University of Azad Jammu and Kashmir, 13100, Muzaffarabad, Pakistan.

[7]PLASMANT research group, NANOLab Center of Excellence, University of Antwerp, Universiteitsplein 1, 2610 Antwerp, Belgium

[8]Institute of Ion-Plasma and Laser Technologies, Academy of Sciences of the Republic of Uzbekistan, 33 Durmon Yuli Street, Tashkent 100125, Uzbekistan

*Email: cii_raj@yahoo.com

*Phone #: +92333-9698704

Abstract:

The synthesis of zinc stannate nanocomposite (Zn_2SnO_4 NC) was carried out using an environment friendly process that included the use of *Ficus carica* (*F. carica*) leaves extract as a capping and reducing agent. X-ray diffraction (XRD) analysis was used to analyze the structural and crystallographic parameters, and the crystallite was discovered to have cubic geometry. The elemental composition of the studied Zn_2SnO_4 NC was investigated using energy dispersive X-

ray (EDX), which revealed that it was extremely pure. The band gap (3.12 eV) was calculated through Tauc plot using diffuse reflectance (DRS) data where the functional groups were explored through Fourier transform infrared (FTIR) spectroscopy. Prior to the photocatalytic reaction, some preliminary experiments were performed, which proposed that pH 9 is suitable for the mineralization of methylene blue (MB) (10 ppm) in the presence of 20 mg of Zn_2SnO_4 NC and simulated solar light. The 96 % of MB was degraded in 80 min with the degradation rate of 0.038 min^{-1}.

Keywords: Environment; Methylene blue; Zinc stannate; Photocatalysis; Degradation.

1. Introduction

The environmental pollution are mainly attributed to the diversifying urbanization and industrialization. Water and soil pollution is caused by the industrial effluents that have been discharged into environment, having negative impacts on all living organism [1]. The high concentration of chemicals, dyes and heavy metals are released into water bodies from dyeing industries polluting the ground and surface water and make it unfit for drinking [2]. Water adulteration via dye discharge from several industries (food processing, paints, cosmetics, textile dyeing, paper making) has captivated major attention because of risk to ecosystem and public health [3]. The making of synthetic dyes is above 7 lac tons/year and greater than 15% of this synthetic colorant is expelled into water per annum and are proved to be mutagenic, xenobiotic and carcinogenic to living organisms [4]. Dyes effluents from the industries like cosmetic, food, dye synthesis, pulp mill, electroplating, textile, paper, and printing are caused water pollution. The xenobiotic properties and complicated aromatic structure of dyes form them arduous to mineralize. A few of the organic dyes and their related products have mutagenic and carcinogenic effects on humans. There is an urgent need to treat the dyes before their release into the water bodies [5]. Methylene blue (MB), a cationic dye and has many applications including silk, wood, and dying cotton. However MB is not believed to be extremely noxious but it can produce some detrimental results such as quadriplegia, jaundice, cyanosis, shock, diarrhea, increased heart rate, vomiting, and tissue deathin human being. Consecutively, MB containing wastewater should be managed properly before letting out into the water bodies [6].

Various biological, chemical, and physical techniques are used for the elimination of unwanted hazardous compounds from contaminated water comprising membrane separation, advanced

oxidation, coagulation and adsorption, precipitation, reverse osmosis, and membrane processes [7]. The methods reported to eliminate the dyes from aqueous solution were of physical and chemical nature but these methods are highly expensive and less efficient for the dye degradation. The stability of these dyes is maintained by using chemicals which are toxic in nature and thus add to the toxicity of the environment[8]. Among these, photocatalysis is one of the most important processes. Photocatalysis is widely used for many applications in treatment of wastewater and manifested a fair approach for the abolition of inorganic and organic pollutants including organic dyes, oil leakage, and pesticides that cannot be degraded in natural forms. Nano photocatalysis is a versatile oxidation process, utilized in the eradication of very minute amount of pollutant from air and water streams. It is more efficacious than conventional methods due to the large surface area- to- volume ratio, uniform and controlled particle size, structure, composition. Among nanophotocatalysts, nanocomposites are preferred because they are efficient, economic and easy to synthesize [9]. The binary composites oxides render the electron-hole recombination process thus increasing the photocatalytic activity. Zinc stannate is a tertiary oxide semiconductor having band gap ($\sim$3.6 eV) and termed as zinc tin oxide (ZTO)[10]. The Zn_2SnO_4 depict wide-band semiconductor oxides with the conductivity of n-type, (transparent within the visible light region), they are optimistic for applications in the fields of gas sensors, lithium-ion batteries, solar cells, transparent conductors, lead-free ferroelectrics and photo catalysis[11]. Depending on the molar ratio of the primary components (Sn, Zn and O), this material exists in two states: $ZnSnO_3$ of the perovskite-type structure and Zn_2SnO_4 of the spinel-type structure[12]. Different approaches are used for the preparation of zinc stannate nanocomposite including thermal evaporation calcinations, sol-gel synthesis, mechanical grinding, hydrothermal, and ion-exchange methods. However, these methods not user friendly due to the wide use of toxic chemical reagents and expensive instruments(Baruah sand Dutta 2011). The green method is one of the most effective, safe and low cost process and is a possible alternate of the conventional methods[14].

The present study was conducted to mineralize MB from aqueous solution on illumination of simulated solar light irradiation using Zn_2SnO_4 NC as photocatalyst. The Zn_2SnO_4 NC was synthesized via ecofriendly and economic process using *F. carica* leaves extract which belongs to the family Moraceae [15]. The physicochemical properties was analyzed through FTIR, DRS, EDX, XRD, and SEM techniques. The photocatalytic degradation of MB was examined under

the effects of initial concentration, pH and catalyst dose. The stability of the Zn_2SnO_4 NC as photocatalyst was also evaluated for several stage degradation process.

2. Materials and Methods

2.1. Materials

Analytical-grade chemicals were used in this research work. The zinc chloride dihydrate, tin chloride dihydrate, sodium hydroxide, and methylene blue were given by Sigma Aldrich and were used without further purification. All of the requisite solutions were made with deionized water. The botany department classified the *F. carica* leaves that were collected from the chemistry department's lawn.

2.2. Preparation of Extract

The *F. carica* leaves were picked, washed in deionized water to remove dust, and then dried in the shade. To make the extract, 50 g of dried leaves were placed in an airtight jar with 1000 mL boiled and deionized water and left for 24 hours. The crude extract was then purified and centrifuged for 10 minutes at 4000 rpm, with the upper layer being saved for future experiments.

2.3. Synthesis of Zn_2SnO_4 NC

For the fabrication of Zn_2SnO_4 NC, the calculated amount (1.05 g) of $ZnCl_2.2H_2O$ was solvated in 50 mL deionized water and 20 mL of the prepared plant extract was introduced. The pH of the reaction mixture was fixed at 10 by dropwise addition 0.1 molar solution of NaOH and was then stirred (250 rpm) and heated (50 °C) for 30 min. The white gel formed was aged at room temperature for 6 h. At the same time, the $SnCl_2.2H_2O$ (0.95 g) was solvated in 50 mL deionized water and 20 mL of the plant extract was introduced and stirred (250 rpm) and heated (50 °C) for 30 min and white gel formed that was aged for 6 h. Afterward, both the gel were mixed with constant stirring (300 °C) and heating (50 °C) for 5 h at room temperature and was then aged for 24 h. The final product was repeatedly washed with deionized water and was oven dried at 150 °C and stored in air tight polyethylene bottle.

2.4. Characterization

The different physicochemical techniques were utilized for the inspection of the structural and surface properties of the synthesized Zn_2SnO_4 NC. The XRD model Panalytical X-Pert Pro was utilized to analyze the crystalline nature of powder. The XRD quantification was made of 20° to 80° in 2θ range and Debye-Scherrer equation was employed for determining the average crystallite size. Morphology was studied by using SEM model JEOL 5910 (Japan). The band gap was determined from data obtained by running DRS (lambda 950) in the 400-1000 nm range using Tauc's plot. The material's elemental analysis was performed on an EDX model INCA200 (UK) operating in the 1-20 keV scale. The FTIR spectrum was recorded using a Nicolet 6700(USA) spectrometer in the range of 4000–400 cm^{-1} [16].

2.5. Photocatalytic activity

During the photocatalytic removal of MB, the photocatalytic behavior of the as-synthesized Zn_2SnO_4 NC was examined. To begin, a 10 ppm MB solution was made in deionized water, and 50 mL of that solution was poured into a reaction vessel, along with 20 mg of Zn_2SnO_4 NC. The reaction mixture was mixed in the dark for 30 min to obtain the adsorption-desorption equilibrium. The solution was then subjected to artificial solar radiation. To extract the catalyst, the 3 mL sample was centrifuged at 4000 rpm for 4 min after a fixed time interval (in min). On a spectrophotometric analysis of the centrifuged sample using a double beam spectrophotometer, the absorbance limit was recorded as a function of time (Thermo Spectronic UV 500).

3. Results and discussion

3.1. Physicochemical study

The diffractogram shown in Fig. 1 possess characteristics Bragg's reflections at 2θ positions with hkl values 30.05(220), 37.32(222), 47.63(331), 50.90 (422), 56.75(511), 57.65(531), 62.70(440), 68.12(620), 70.10(533) and 79.35(622). These bands correspond to those listed in JCPDS card 00-024-1470, which confirm the synthesis of Zn_2SnO_4 NC having Fd3m space group and cubic geometry. The length of three coordinates (a,b and c) of the cubic Zn_2SnO_4 NC are equal to 8.5674 Å whereas the angles alpha, beta and gamma are of 90°. The intense and sharp diffraction bands confirm the formation of well crystalline nanostructures and all peaks were assigned to the desired elements, suggesting the synthesized samples are highly pure. The crystallite size for

Zn$_2$SnO$_4$ NC was quantified by Debye-Scherrer's equation is 42.47 nm along with 0.32 % imperfection was also found in the crystal.

(Position for Fig.1)

The EDX spectrum of Zn$_2$SnO$_4$ NC shown as inset in Fig. 1, exhibits the bands assigned to Sn, Zn and O, which confirm the synthesis of highly pure Zn$_2$SnO$_4$ NC. The peaks in the range of 3.4 to 3.9 keV are attributed to Sn along with a sharp signal at 0.4 keV is credited to O in the sample. The three bands at 1, 8.7 and 9.6 keV are due to the Zn and the weight percentages derived from the EDX data for Zn, Sn, and O are 42.95, 36.33 and 20.71 % respectively. The SEM micrographs (low and high magnification)given in Fig.2, shows randomly arranged intra-particles cavities. The small particles areclosely connected with each other forming larger various shaped structures specially the cauliflower like at the right lower corner of the image (b). On close observation, small individual particles with almost uniform shape are present on the surface of the complex structures. The histogram located on the left corner of image (a) shows two sharp peaks at 50 and 104 suggesting that theparticles size is ranging from 50 to 104 nm with the average of 79 nm.

(Position for Fig. 2)

The electronic state of the Zn$_2$SnO$_4$ NC was calculated using the transmittance spectrum, which indicates that all of the samples are translucent over a broad wavelength range. The band gap energies were determined using the Tauc relation (eq.1), where *B* is constant, *hv* is the light intensity, is the absorption coefficient, and the exponent *n* is depending on the type of transition: direct, forbidden direct, indirect, or forbidden indirect, and can have values of 1/2, 2, 3/2, or 3 respectively [17].

$$\alpha hv = B\left(hv - E_g\right)^n \tag{eq.1}$$

The α and transmittance are correlated as given in eq. 2, where *L* is the thickness of the sample for direct allowed transition (n=1/2), by combining eq. 1 and eq. 2, we have;

$$T = \exp(-\alpha L) \, OR \, \alpha = -\frac{lnT}{L} \tag{eq.2}$$

$$(hvlnT)^2 = B^2 L^2 \left(hv - E_g\right) \tag{eq.3}$$

(Position for Fig. 3)

The band gap energies were calculated for Zn_2SnO_4 NC from Tauc plots by joining sharp rising portion with horizontal axis of the *(hvlnT)²* against *hv* is 3.12 eV [18,19]. The band gap energy for Zn_2SnO_4 NC is divergent from that of SnO_2 NPs and ZnO NPs suggesting that the production of new species and all the deduced band gap energies are in accordance with the reported data [20–25]. In the FTIR spectrum of Zn_2SnO_4 NC (Fig.4), the peaks at 3489.2, 3438.9 and 1634.4 cm^{-1} are because of the deformation, stretching and bending vibrations of adsorbed water molecules[26]. The stretching vibration of O-Sn-O in the lattice system and potential bonding of Zn in ZnO are attributed to the small broad peaks at 1484.53 and 1402.61 cm^{-1}, respectively [22]. The stretching vibrations of ZnO and SnO_2 pairs, which can be due to the Sn-O-Zn bonding in Zn_2SnO_4, are responsible for the peaks at 719.4 and 550.47 cm^{-1} [27].

(Position for Fig.4)

3.2.Photocatalytic study

The photocatalytic potency of Zn_2SnO_4 NC was analyzed to degrade MB with the catalyst concentration of 20mg on irradiating simulated solar light. The visual photodegradation of MB was observed due to the fading of color with the increase in irradiation time. The eq. 4 was used to determine the percentage degradation (Fig. 5), that inferred 96% of the dye was mineralized in 80 min of contact with the catalyst under simulated solar light. The self-photolysis was also performed on irradiation of simulated solar light without introducing catalyst and it was observed that there was a minor reduction of the original concentration of the MB solution which assures the stability of the MB dye. This infers that the Zn_2SnO_4NC is highly effective and the dye would not be degraded without it. The Langmuir-Hinshelwood kinetic model (eq. 5) was applied for the kinetic modeling of the kinetic data where$C$ is the concentration at time (*t*),C_e is the initial concentration whereas *k* is the rate constant. A straight line is obtained by plotting *ln(C/Co)* versus time (*t*) shows that the photocatalytic degradation reaction obeys pseudo first order kinetics and the k value was found to be 0.038 min^{-1}.

$$\% \, Degradation = \frac{Ct - Co}{Co} \times 100 \qquad\qquad (eq.4)$$

$$\ln(C/Co) = -kt \qquad\qquad (eq.5)$$

(Position for Fig. 5)

Dosage study

The 10 ppm MB was exposed different quantities of the Zn_2SnO_4 NC (5, 10, 15, 20, 25 and 30 mg) to check the affect of catalyst dosage on the catalytic mineralization process. From the experiment Fig. 6(A), it was inferred that the degradation of MB increases with increasing the dose of catalyst up to 20 mg while further elevation in the dose reduced the degradation process. This decrease in the degradation is attributed to the phenomenon of deactivation of catalyst. When large amount of catalyst is introduced to the solution collision ensues between the activated and the ground state catalyst that leads to the deactivation of the activated molecules and consequently degradation decreases [28].

3.2.1. Initial concentration study

In the present work, 5, 10, 20, 30 and 40 ppm MB solutions were unveiled to the Zn_2SnO_4 NC to scrutinize the effect of dye concentration on the photocatalytic mineralization. The results shows Fig. 6(B)that the degradation increases with increasing initial concentration of MB up to 10 ppm whereas gradual decrease was observed with increasing initial concentration. On increasing dye concentration the MB molecules begin to absorb light and so the catalyst cannot absorb sufficient light and thus the dye removal efficiency of the catalyst reduced. This also because of the adsorption of large number of MB molecules on the surface of Zn_2SnO_4 NC at higher concentration results into the blocking of the active sits and thus reduce the degradation[28].

3.2.2. pH study

The pH of the solution is the key parameter that significantly affects surface properties of catalyst. The pH study on photocatalytic degradation of MB was evaluated in pH range of 3 to 11 using 10 ppm dye solution and exposed 20 mg of Zn_2SnO_4 NC as shown in Fig. 6(C). The upshots inferred that the percentage degradation of MB was maximum at pH 9 as compared to other studied pH. MB being a cationic dye shows maximum degradation in the alkaline medium and maximum degradation is exhibited at pH 9 and the activity decreased with further increased. The enhanced activity at pH is attributed to formation of hydroxyl ions that are accountable for

the production of hydroxyl radicals. The low degradation at pH 11 is might be due to the dissociation of Zn_2SnO_4 NC, thus optimum pH for the degradation of MB is 9[29].

3.2.3. Reusability study

The stability of the Zn_2SnO_4 NPs in term of its reusability was analyzed against the five-fold degradation of the MB. The experiment was performed by the addition of fresh MB solution by degrading the previous one under same conditions for five times. The Fig. 6(d) shows that there is a negligible reduction in the efficiency of the Zn_2SnO_4catalystafter three cycles and decrease on the efficiency of the catalyst that is ascribed to the surface coverage of the catalyst. Overlooking to the photocatalytic efficiency, the Zn_2SnO_4NCis the most appropriate catalyst to be used for degradation of organic pollutants under simulated solar light and it can be effectively used for various stage reactions.

(Position for Fig. 6)

3.2.4. Photocatalytic mechanism

Photocatalysis is a kind of reaction that proceeds on the expense of energy that is equal or higher than the band gap of the catalyst. The electrons move from the valance band to the conduction band on irradiating of semiconductor with a light source. After effect equal number of holes are engendered in valence band. All types of microbial, organic, and inorganic contaminants owing to their redox potential are degrading via photo-generated holes and electrons. They react with adsorbed electron acceptors and electron donors by migrating to the surface to produce hydroxyl radicals, hydrogen peroxides, superoxide radical anions. The hydroxyl radical reacts with aqueous solution resultantly producing innocuous compounds. Under same reaction conditions, the organic pollutants are thoroughly oxidized to halide ions, H_2O and CO_2 on negligible production of displeasing by-products [9]. In the present study, the reaction mixture was irradiated with the simulated solar light and the electrons of both the oxides get excited to conduction and the holes are generated in the valance band. The electrons and the holes are adequately separated as the holes get assembled in the VB of ZnO while they were generated in the VB of SnO_2 similarly, electrons get shifted to the CB of SnO_2 from the CB of ZnO. Later the $^\bullet OH$ and $O_2^{-\bullet}$ are produced by the reaction of holes (h^+) and electrons (e^-) with the water and

absorbed oxygen respectively. The $O_2^{-\bullet}$ free radical serve as an additional source of producing $^\bullet OH$ radicals which then lead to the degradation of the MB to non-toxic material [16].

4. Conclusion

The manipulation of plant materials for the fabrication of nanomaterials is the most effective, economical and nontoxic route. The investigated physicochemical properties confirm the highly crystalline nature of Zn_2SnO_4 NC with band gap of 3.13 eV was found most efficient catalyst for the photodegradation of MB. The operational parameters like pH, initial concentration of MB and catalyst dose govern the photocatalytic mineralization of MB. The photocatalytic reaction was found to follow first order kinetic and 96 % MB was deteriorated in 80 min with the rate of degradation 0.038 min^{-1} at pH 9 and catalyst dose of 20 mg. This study reveals that the Zn_2SnO_4 NC is an efficient, economical and stable photocatalyst for the remediation of organic pollutants.

References

[1]   A. Salama, A. Mohamed, N.M. Aboamera, T.A. Osman, A. Khattab, Photocatalytic degradation of organic dyes using composite nanofibers under UV irradiation, Applied Nanoscience (Switzerland). 8 (2018) 155–161. doi:10.1007/s13204-018-0660-9.

[2]   D.N. S, Impact of Dyeing Industry Effluent on Groundwater Quality by Water Quality Index and Correlation Analysis Journal of Pollution Effects & Control, 2 (2014) 2–5. doi:10.4172/2375-4397.1000126.

[3]   P. Zhu, Z. Ren, R. Wang, M. Duan, L. Xie, J. Xu, Preparation and visible photocatalytic dye degradation of, 14 (2020) 33–42.

[4]   H. Anwer, A. Mahmood, J. Lee, K. Kim, J. Park, A.C.K. Yip, Photocatalysts for degradation of dyes in industrial effluents : Opportunities and challenges, 12 (2019) 955–972.

[5]   T. Liu, Y. Li, Q. Du, J. Sun, Y. Jiao, G. Yang, Z. Wang, Y. Xia, W. Zhang, K. Wang, H. Zhu, D. Wu, Adsorption of methylene blue from aqueous solution by graphene, Colloids and Surfaces B: Biointerfaces. 90 (2012) 197–203. doi:10.1016/j.colsurfb.2011.10.019.

[6]   Y. Li, Q. Du, T. Liu, X. Peng, J. Wang, J. Sun, Y. Wang, S. Wu, Z. Wang, Y. Xia, L. Xia,

Comparative study of methylene blue dye adsorption onto activated carbon, graphene oxide, and carbon nanotubes, Chemical Engineering Research and Design. 91 (2013) 361–368. doi:10.1016/j.cherd.2012.07.007.

[7]   M. Fakhrzad, A.H. Navidpour, M. Tahari, S. Abbasi, Synthesis of Zn2SnO4 nanoparticles used for photocatalytic purposes, Materials Research Express. 6 (2019). doi:10.1088/2053-1591/ab2eb5.

[8]   I. Khan, K. Saeed, I. Khan, Nanoparticles : Properties , applications and toxicities, Arabian Journal of Chemistry. 12 (2019) 908–931. doi:10.1016/j.arabjc.2017.05.011.

[9]   V.C. Padmanaban, M.S. Giri Nandagopal, G. Madhangi Priyadharshini, N. Maheswari, G. Janani Sree, N. Selvaraju, Advanced approach for degradation of recalcitrant by nanophotocatalysis using nanocomposites and their future perspectives, International Journal of Environmental Science and Technology. 13 (2016) 1591–1606. doi:10.1007/s13762-016-1000-9.

[10]   S. Danwittayakul, M. Jaisai, T. Koottatep, J. Dutta, Enhancement of photocatalytic degradation of methyl orange by supported zinc oxide nanorods/zinc stannate (ZnO/ZTO) on porous substrates, Industrial and Engineering Chemistry Research. 52 (2013) 13629–13636. doi:10.1021/ie4019726.

[11]   S. Sagadevan, J. Singh, K. Pal, Z. Zaman, Hydrothermal synthesis of zinc stannate nanoparticles spectroscopic investigation, Journal of Materials Science: Materials in Electronics. 0 (2017) 0. doi:10.1007/s10854-017-6916-4.

[12]   S.S. Nalimova, A.I. Maksimov, L.B. Matyushkin, V.A. Moshnikov, Current State of Studies on Synthesis and Application of Zinc Stannate (Review), 45 (2019) 251–260. doi:10.1134/S1087659619040096.

[13]   S. Baruah, J. Dutta, Zinc Stannate Nanostructures : Hydrothermal Synthesis Zinc stannate nanostructures : hydrothermal synthesis, (2011). doi:10.1088/1468-6996/12/1/013004.

[14]   V.N. Kalpana, V.D. Rajeswari, A Review on Green Synthesis , Biomedical Applications , and Toxicity Studies of ZnO NPs, 2018 (2018).

[15]   C.M. Chetty, Antioxidant Properties of Ficus Species – A Review, 2 (2010) 2174–2182.

[16]   S. Shoukat, W. Rehman, S. Haq, M. Waseem, A. Shah, Synthesis and characterization of zinc stannate nanostructures for the adsorption of chromium (VI) ions and photo-degradation of rhodamine 6G, Materials Research Express. 6 (2019) 1–12. doi:10.1088/2053-1591/ab473c.

[17]   M. Dehbashi, M. Aliahmad, Experimental study of structural and optical band gap of nickel doped tin oxide nanoparticles, International Journal of Physical Sciences. 7 (2012) 5415–5420. doi:10.5897/IJPS11.1606.

[18]   F. Gu, S.F. Wang, C.F. Song, M.K. Lü, Y.X. Qi, G.J. Zhou, D. Xu, D.R. Yuan, Synthesis and luminescence properties of SnO2 nanoparticles, Chemical Physics Letters. 372 (2003) 451–454. doi:10.1016/S0009-2614(03)00440-8.

[19]   V. Vinoth, T. Sivasankar, A.M. Asiri, J.J. Wu, K. Kaviyarasan, S. Anandan, Photocatalytic and photoelectrocatalytic performance of sonochemically synthesized Cu2O@TiO2 heterojunction nanocomposites, Ultrasonics Sonochemistry. 51 (2018) 223–229. doi:10.1016/j.ultsonch.2018.10.022.

[20]   B. Venugopal, B. Nandan, A. Ayyachamy, V. Balaji, S. Amirthapandian, B.K. Panigrahi, T. Paramasivam, Influence of manganese ions in the band gap of tin oxide nanoparticles: structure, microstructure and optical studies, RSC Advances. 4 (2014) 6141. doi:10.1039/c3ra46378h.

[21]   B. Baruwati, D.K. Kumar, S. V. Manorama, Hydrothermal synthesis of highly crystalline ZnO nanoparticles: A competitive sensor for LPG and EtOH, Sensors and Actuators, B: Chemical. 119 (2006) 676–682. doi:10.1016/j.snb.2006.01.028.

[22]   M. Zhang, T. An, X. Hu, C. Wang, G. Sheng, J. Fu, Preparation and photocatalytic properties of a nanometer ZnO-SnO 2 coupled oxide, Applied Catalysis A: General. 260 (2004) 215–222. doi:10.1016/j.apcata.2003.10.025.

[23]   M.B. Ali, F. Barka-Bouaifel, H. Elhouichet, B. Sieber, A. Added, L. Boussekey, M. Ferid, R. Boukherroub, Hydrothermal synthesis , phase structure , optical and photocatalytic

properties of Zn2SnO4 nanoparticles, Journal of Colloid And Interface Science. 457 (2015) 360–369. doi:10.1016/j.jcis.2015.07.015.

[24] S. Haq, W. Rehman, M. Waseem, R. Javed, Mahfooz-ur-Rehman, M. Shahid, Effect of heating on the structural and optical properties of TiO2 nanoparticles: antibacterial activity, Applied Nanoscience. 8 (2018) 11–18. doi:10.1007/s13204-018-0647-6.

[25] A.N. Naje, A.S. Norry, A.M. Suhail, Preparation and Characterization of SnO 2 Nanoparticles, Int. J. Innov. Res. Sci. Eng. Technol. 2 (2013) 7068–7072. doi:10.1088/0957-4484/13/5/304.

[26] S. Haq, S. Shoukat, W. Rehman, M. Waseem, A. Shah, Green fabrication and physicochemical investigations of zinc-cobalt oxide nanocomposite for wastewater treatment, Journal of Molecular Liquids. 318 (2020) 114260. doi:10.1016/j.molliq.2020.114260.

[27] M.M. Rashad, A.A. Ismail, I. Osama, I.A. Ibrahim, A.H.T. Kandil, Photocatalytic decomposition of dyes using ZnO doped SnO$_2$ nanoparticles prepared by solvothermal method, Arabian Journal of Chemistry. 7 (2014) 71–77. doi:10.1016/j.arabjc.2013.08.016.

[28] S. Alkaykh, A. Mbarek, E.E. Ali-Shattle, Photocatalytic degradation of methylene blue dye in aqueous solution by MnTiO$_3$ nanoparticles under sunlight irradiation, Heliyon. 6 (2020) e03663. doi:10.1016/j.heliyon.2020.e03663.

[29] T. Nguyen, T. Thu, N.N. Thi, V.T. Quang, K. Nguyen, Synthesis , characterisation , and effect of pH on degradation of dyes of copper-doped TiO$_2$, Journal of Experimental Nanoscience. 11 (2016) 226–238. doi:10.1080/17458080.2015.1053541.

List of Figures

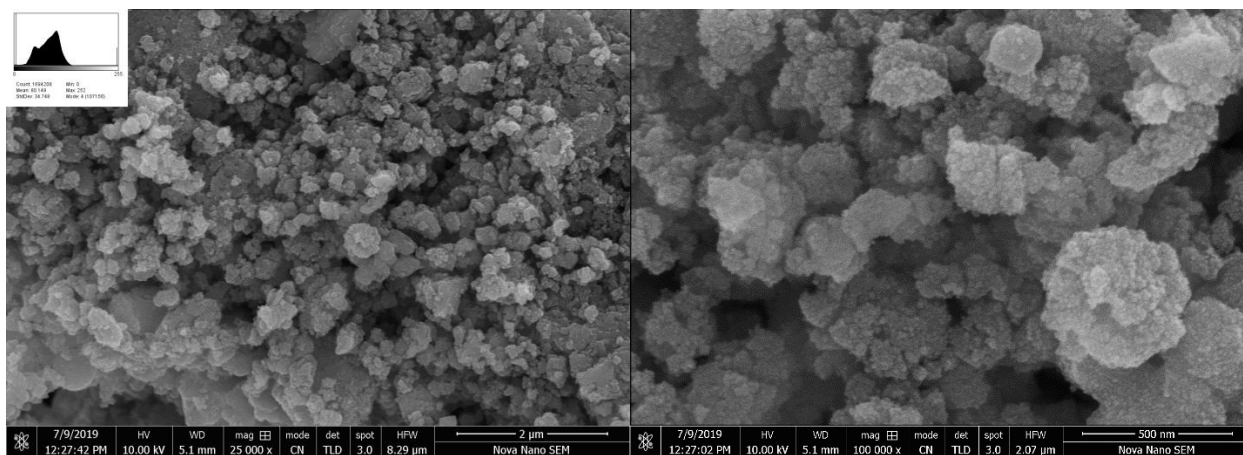Fig. 1: XRD diffractogram (inset: EDX spectrum) of Zn_2SnO_4 NC

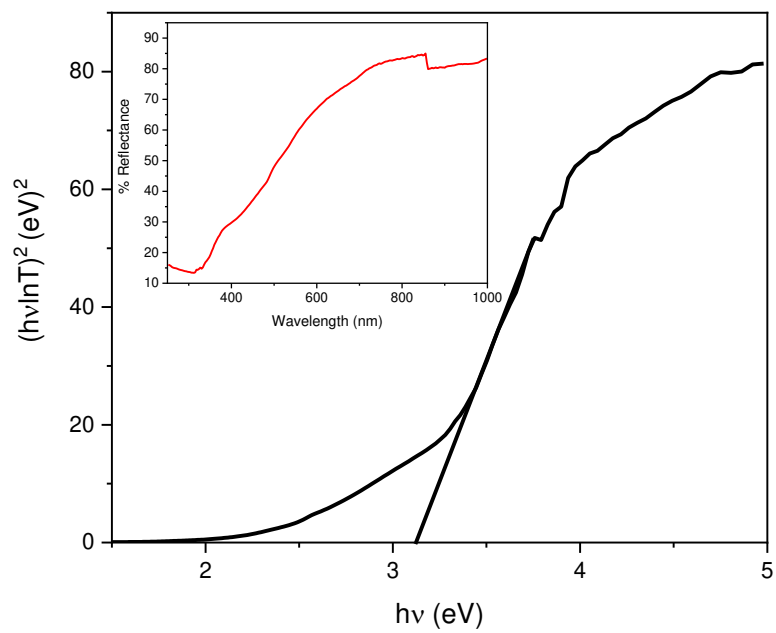Fig. 2: Low (a) (inset: histogram) and High (b) magnification SEM micrographs of Zn_2SnO_4 NC

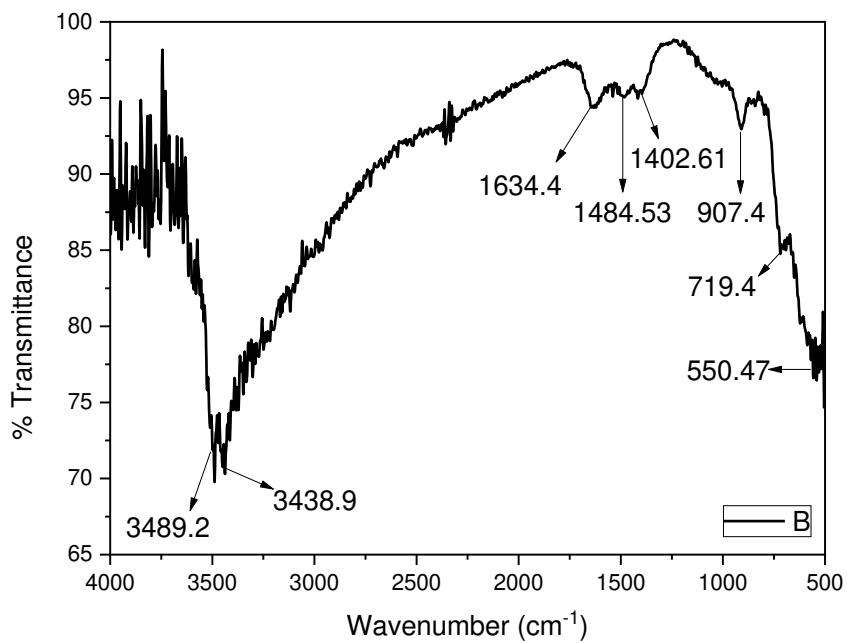Fig. 3: Tauc's plot (inset: DRS spectrum) of Zn_2SnO_4 NC
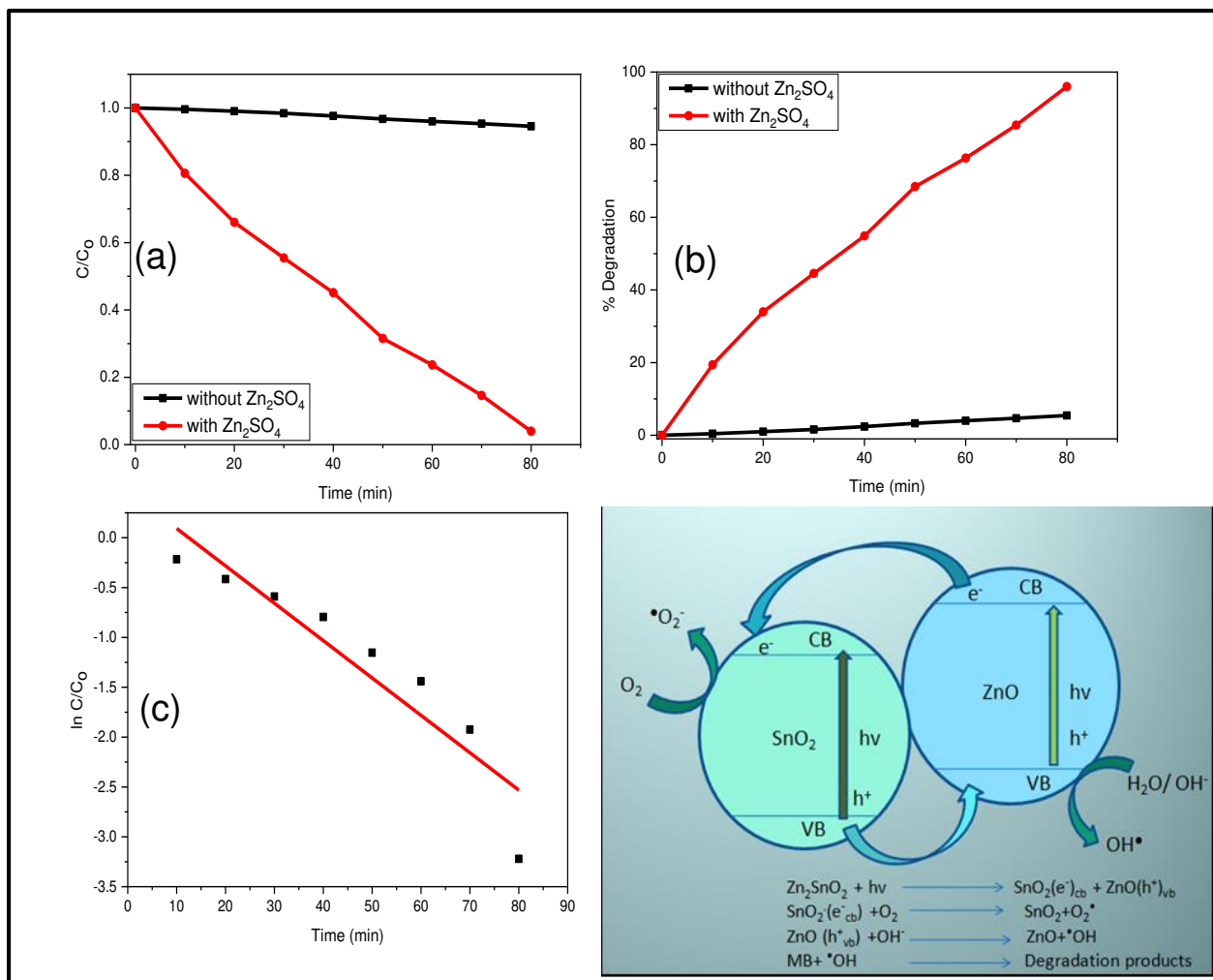

Fig. 4: FTIR spectrum of Zn_2SnO_4 NC

Fig. 5: Degradation profile (C/C$_o$) (a), percentage degradation (b), kinetic plot (c) and schematic degradation mechanism of MB in the presence of Zn$_2$SnO$_4$ NC
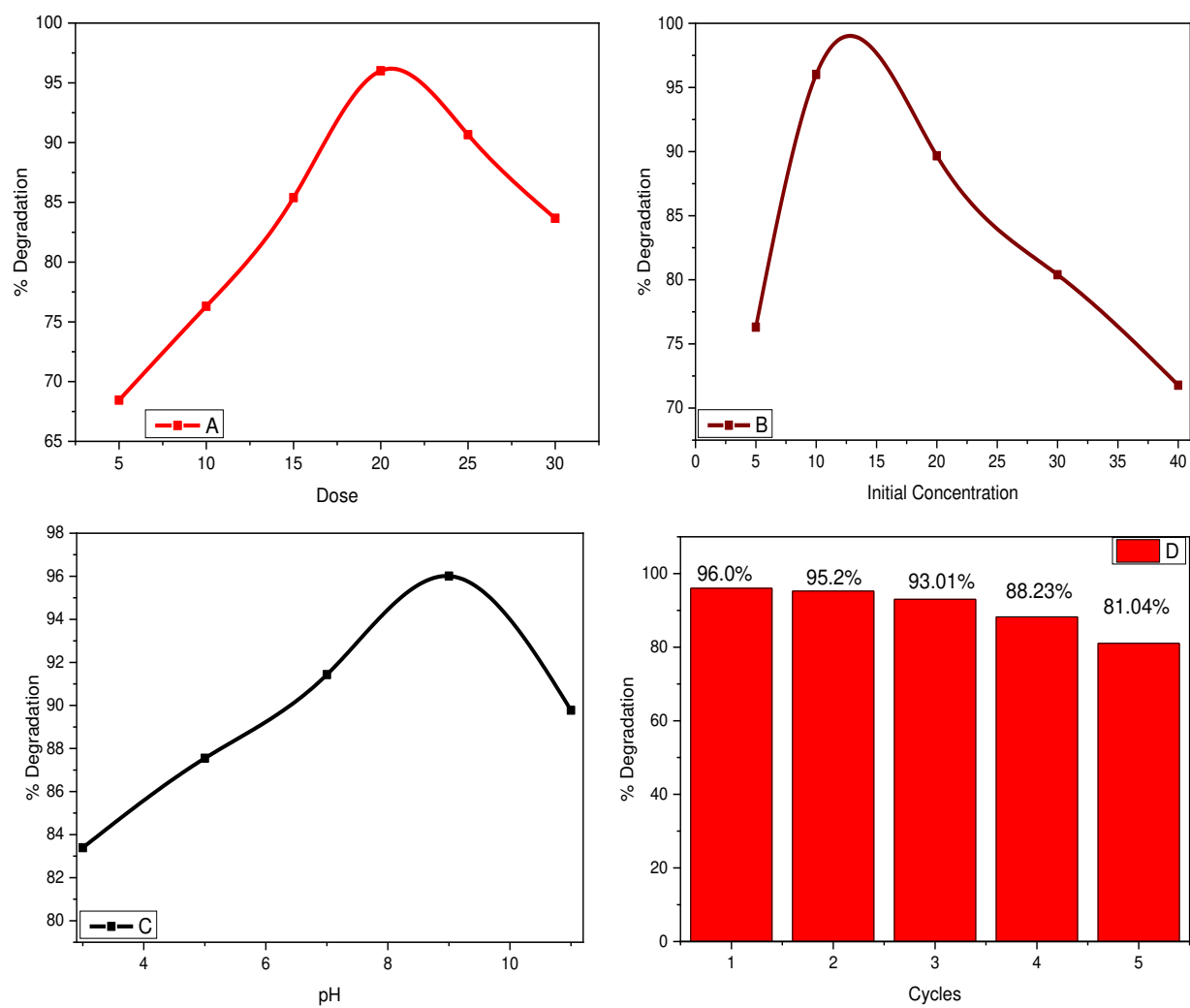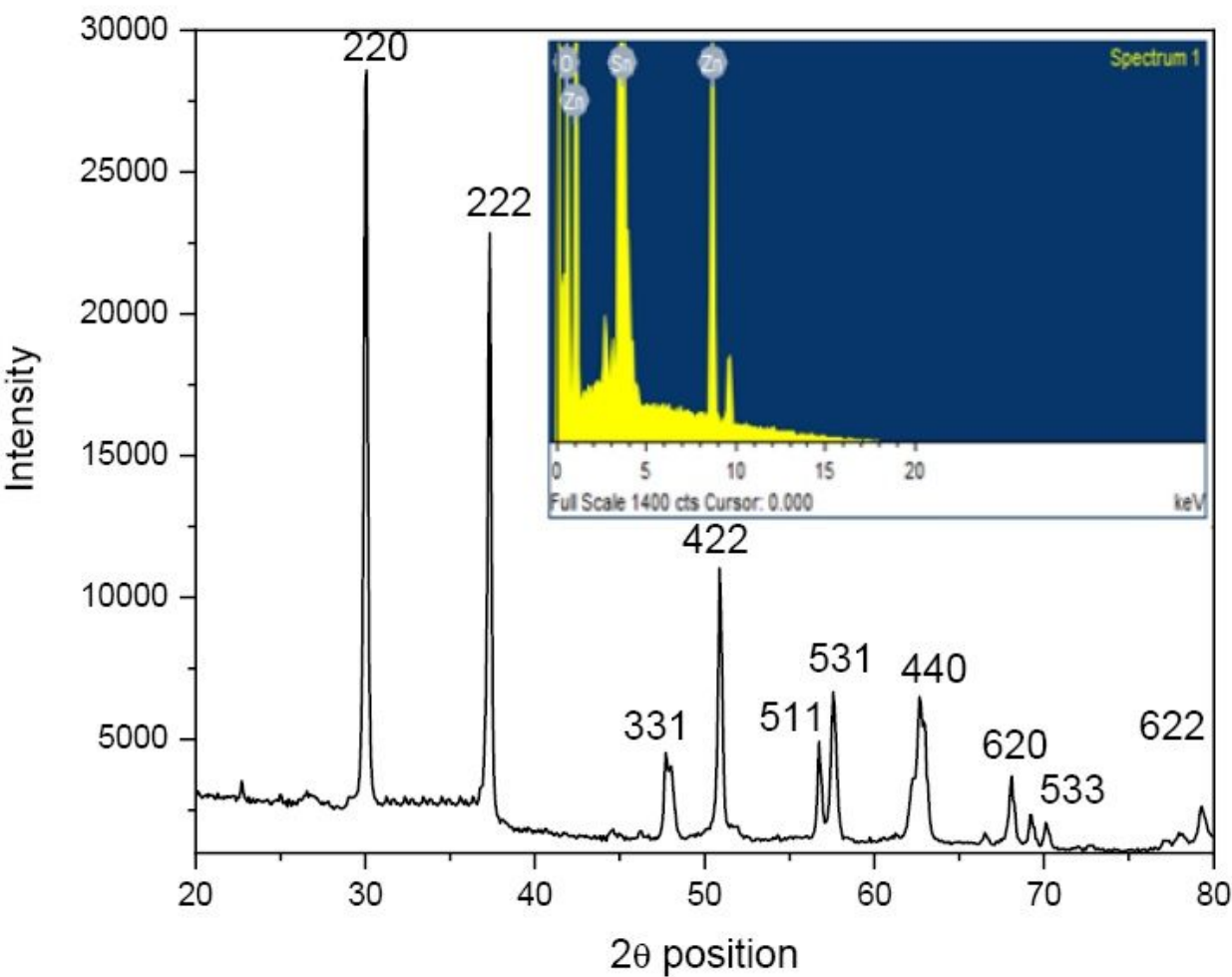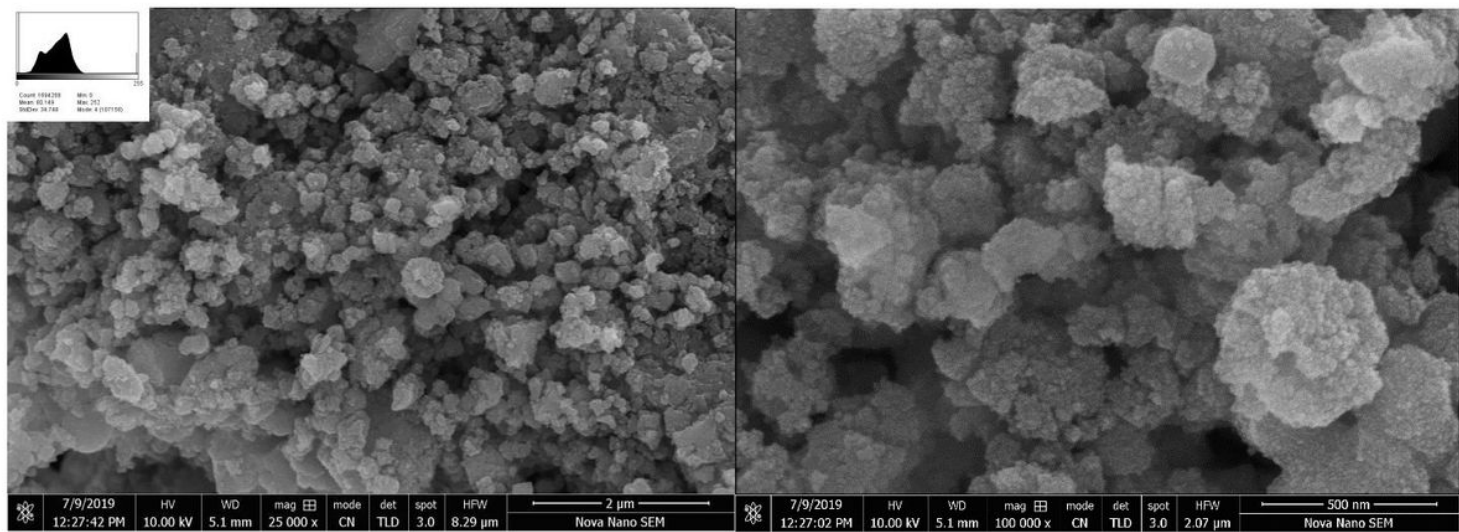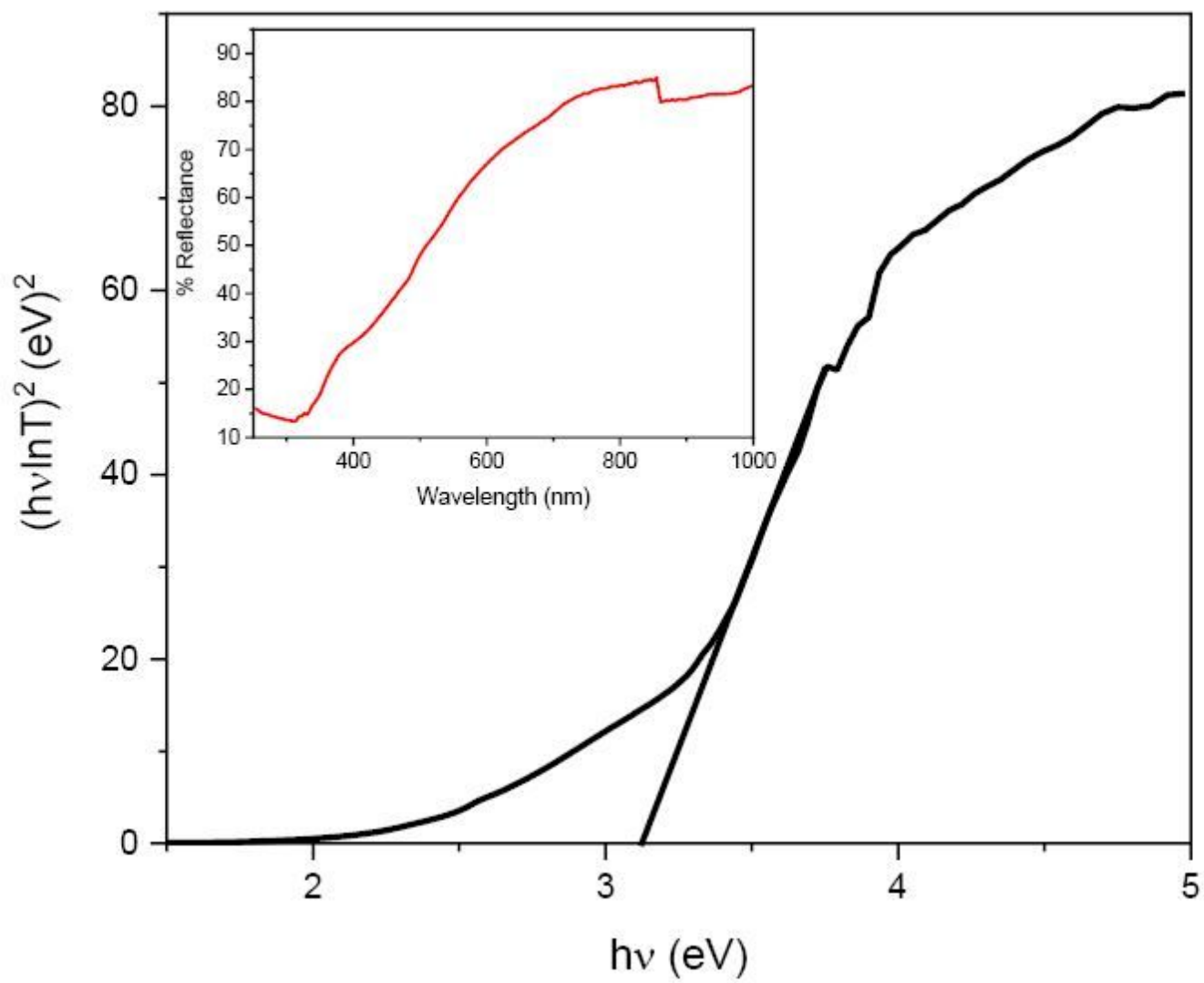
Fig. 6: percentage degradation of MB at different catalyst dose (a), initial concentration (b), pH (c) and cycles (d) of photocatalytic degradation.

Figures

Figure 1

XRD diffractogram (inset: EDX spectrum) of Zn2SnO4 NC

Figure 2

Low (a) (inset: histogram) and High (b) magnification SEM micrographs of Zn2SnO4 NC

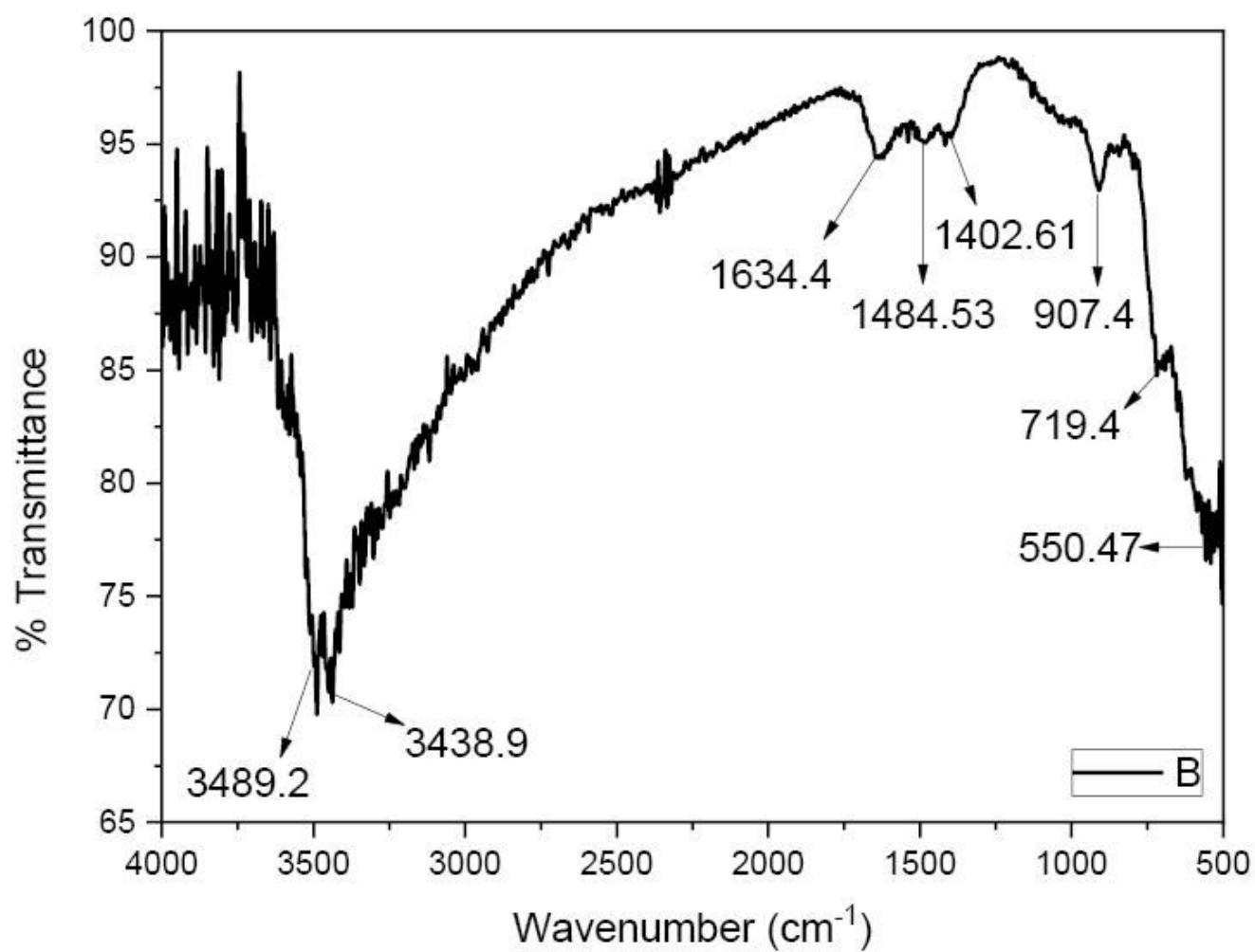**Figure 3**

Tauc's plot (inset: DRS spectrum) of Zn2SnO4 NC
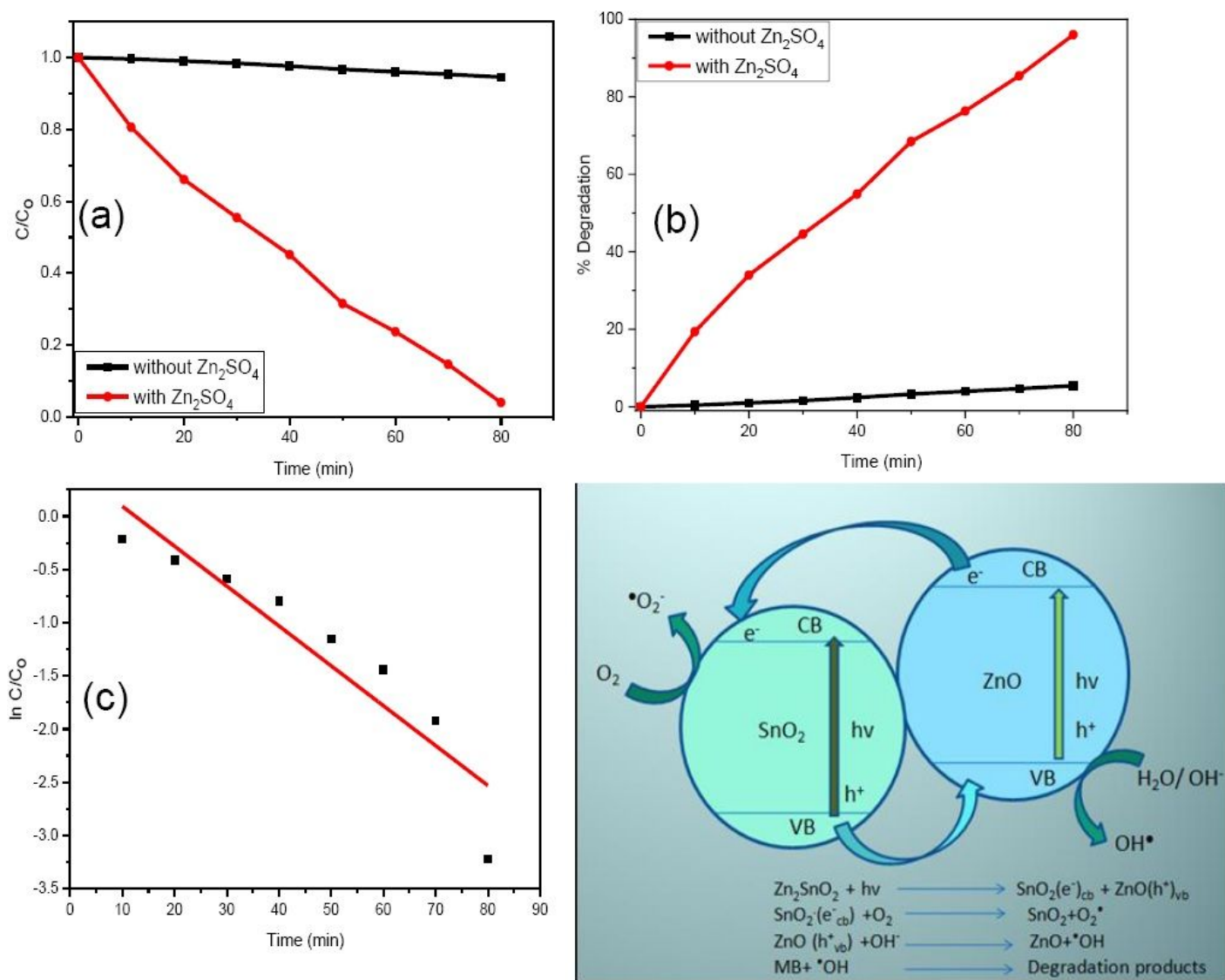
Figure 4

FTIR spectrum of Zn2SnO4 NC

Figure 5

Degradation profile (C/Co) (a), percentage degradation (b), kinetic plot (c) and schematic degradation mechanism of MB in the presence of Zn2SnO4 NC
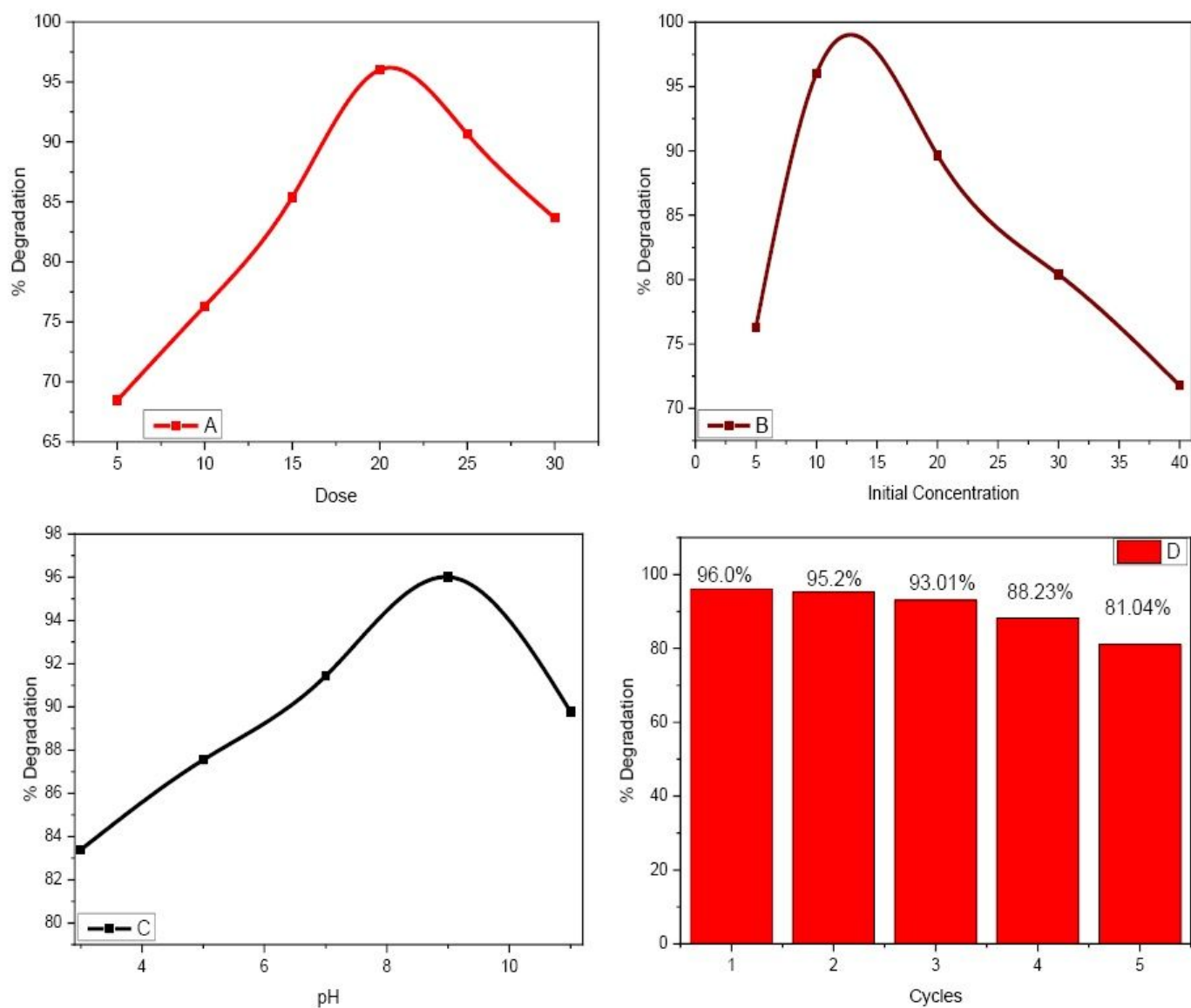
Figure 6

percentage degradation of MB at different catalyst dose (a), initial concentration (b), pH (c) and cycles (d) of photocatalytic degradation.